JOURNAL OF NANO AND MATERIALS SCIENCE RESEARCH
Volume 1 (Maiden edition, 2022), pp. 16-21
Available online at journals.nanotechunn.com/jnmsr

ORIGINAL ARTICLE

Dye Sensitized Solar Cells with Silver Nanoparticles in Nanocomposite Photoanode for Exploring Solar Energy Concept

Jamila Tasiu[a], Eli Danladi [b], Mary T. Ekwu[c] and Lucky Endas[d]*

[a]*Department of Physics, Kaduna State University, Kaduna, Nigeria*
[b]*Department of Physics, Federal University of Health Sciences, Otukpo, Benue State, Nigeria*
[c]*Department of Physics, Airforce Institute of Technology, Kaduna, Nigeria*
[d]*Department of Chemical Sciences, Greenfield University, Kaduna, Nigeria*

KEYWORDS

DSSCs,
Surface plasmon,
Nanoparticles,
Natural pigment

ARTICLE HISTORY

Received: July 3, 2022
Revised: July 18, 2022
Accepted: August 2, 2022

ABSTRACT

Surface plasmon resonance is the effect of electron oscillation in a structure stimulated by incident light. When noble materials such as Ag, Au or Cu are added into the titania (compact or mesoporous) structure of the dye sensitized solar cell (DSSCs), the plasmonic effect of such materials will result to an improved performance of the device. Placing Silver Nanoparticles (AgNPs) at different position will produce a variety of result. In this work the systematic formation of plasmonic dye sensitized solar cells by integrating Ag nanoparticles in two distinct configurations; on the Compact Titanium dioxide (c-TiO_2) and on Mesoporous Titanium dioxide (m-TiO_2) were reported. The Power Conversion Efficiency (PCE), Current density (J_{sc}) and Open circuit voltage (V_{oc}) of the reference device shows a value of 0.36 %, 1.89 $mAcm^{-2}$ and 0.45 V. Upon introduction of AgNPs on the c-TiO_2, a PCE of 0.64 %, J_{sc} of 2.53 $mAcm^{-2}$ and V_{oc} of 0.46 V were recorded, which improved the PCE ~ 63.90 % over that of the pristine device. When AgNPs was introduced on the m-TiO_2, a PCE of 0.71 %, J_{sc} of 2.83 $mAcm^{-2}$ and V_{oc} of 0.46 V were obtained which results to increase in power conversion efficiency from 0.36 % to 0.71 %, demonstrating ~1.97 times enhancement, compared with the reference device without the metal NPs. The improvement is attributed to an increase in photocurrent density due to enhanced light harvesting by silver nanoparticles.

1 Introduction

The issue of energy can be seen as a necessity being a critical problem facing the world and humanity today. As the earth receives abundant energy from the sun, it is wise for such abundant energy to be harvested. Solar cell is one of the means to directly harness such energy. Sequentially, the solar cell technologies have existed in three different types otherwise called generations [1, 2].

The first-generation photovoltaic solar cell is based on a single crystalline semiconductor wafer. The second era solar cells use thin layer of polycrystalline semiconductor, they are less expensive to produce, adaptable and lightweight; however, the performance is still lower than the first-generation cells. The third era solar cell is a new minimal chemical solar cell that was accomplished by the combination of nanostructured electrodes and proficient charge injection dyes [3, 4].

The recent developments in dye sensitized solar cells have created high hope in the renewable energy field due to their ease of fabrication and low cost [5-8]. To date, the highest reported efficiency of DSSC is about 14.3% [9, 10]. Recently, solar cell structure with perovskite nanocrystal as sensitizer has emerged as a new breakthrough in the solar cells field where efficiency as high as >25% has been reported [11, 12].

The main working mechanism of DSSC relies on the photon absorption by the sensitizer followed by the transfer of photogenerated electrons within the circuit. However, increasing power conversion efficiency further to make it an

*CORRESPONDING AUTHOR | Eli Danladi | ✉danladielibako@gmail.com

appealing technology for deployment is still one of the crucial issues in DSSC research. The absorption process can be enhanced with the inclusion of noble metal nanoparticles in the TiO_2 compact and mesoporous structure, acting as scattering centers and sub-wavelength antennas [13].

It is worth mentioning that for noble metal nanoparticles to have significant positive effect in solar cells, the non-radiative transfer between the photoactive layer and nanoparticles must be reduced [3, 14]. Noble materials such as Ag, Cu or Au nanoparticles are thought to enhance the photocurrents of DSSC as a result of localized surface plasmon resonance (LSPR) effect of the nanoparticles [15, 16].

In general, LSPR is the effect of electron oscillation in a structure that is being stimulated by incident light. The effect of the LSPR on noble metal nanoparticles results in enhanced light absorption and scattering which ultimately enhances the performance of DSSCs. This effect was previously demonstrated [16], through introducing AgNPs@TiO_2 on the FTO and on the TiO_2. The study showed that, for efficient device performance, the AgNPs@TiO_2 is placed on the TiO_2. With this, it is important to explore the influence that AgNPs has on dense and mesoporous nanostructure so as to make inference on the performance of DSSCs.

In this work, we demonstrated the influence of silver nanoparticles deposited on the compact-TiO_2 and mesoporous-TiO_2 on the photovoltaic performance of DSSCs. The choice of Ag over other noble metal nanoparticles was attributed to its high conduction, chemical and thermal stability [13]. The devices were developed based on *delonix regia* as the photosensitizer in a sandwich architecture.

2 Materials and Methods

2.1 Synthesis of Ag nanoparticles

Silver nanoparticles was synthesized using a method previously described [16, 17, 18]. This method has to do with mixing sodium borohydride and tri-sodium citrate. The mixing was achieved in the ratio of 2:7. This followed by heating to 60 ℃ at 300 rpm for 40 mins. Under this condition, the mixture was vigorously stirred for uniform formation of the solution. 4 ml of an aqueous solution of $AgNO_3$ was added dropwise to the mixture, after 40 mins of stirring. With that, the temperature was raised to 100 ℃ The reaction was maintained for further 45 mins. The solution was made to cool to room temperature. The silver nanoparticles were collected by process of centrifugation at 5000 rpm after which it was re-dispersed in ethanol via sonication process for 15 mins.

2.2 Extraction of dye pigment

The *delonix regia* flower was collection from the flame tree and blended using an electronic blender with 100 ml distilled water. The sample was filtered to remove the residue and stored in test tubes. The filtrate (extract) was the dye solution used for the sensitization.

2.3 Solar Cells Preparation

Fluorine doped tin oxide (FTO) with sheet resistance of 8 Ω square^{-1} was used as a transparent glass for both photoanode and counter electrode. 0.38 M di-isopropoxytitanum bis (acetylacetonate) in ethanol was spin-coated at 2500 rpm for 15 seconds. This was followed by sintering at 450 ℃ for 30 mins to form a compact layer. The mesoporous layer of the TiO_2 was deposited via screen printing technique. It was then sintered in air for 30 mins at 500 ℃.

For photoanode with silver nanoparticles, the Ag nanoparticles was deposited on the c-TiO_2 and m-TiO_2 using dip coating procedure. To ensure homogeneous distributed of the AgNPs on c-TiO_2 and m-TiO_2, it was sonicated for 20 minutes. The as-prepared photoanodes were soaked overnight in 0.2 mM *delonix regia* dye.

Counter electrodes were prepared by spin coating a platinum (Pt) film on FTO. The Pt coated FTO was then sintered at 500 ℃ for 30 mins.

The iodide-based liquid electrolyte was prepared following the method earlier described by Jun et al [1]. Solar cell assembly was done by sandwiching the liquid electrolyte between the sensitized electrode and Pt counter electrode.

2.4 Characterization and Measurement

Optical study of the dye, electrodes without dye and electrodes with dye were recorded on Axiom Medicals (UV752 UV-Vis-NIR spectrophotometer). Scanning Electron Microscopy (SEM) images were obtained using Phenom pro-X at an acceleration voltage of 10 kV. Structural analysis of the TiO_2 film was performed using X-ray diffractometer (Rigaku D, Max 2500). The current density-voltage characteristics of the cells were recorded using a setup comprising a xenon lamp, an AM 1.5 light filter, and an Electrochemical Analyzer (Keithley-2400 source meter) under an irradiance of 100 mW/cm^2 illumination. The cells active area was 0.50 cm^2.

3 Results and Discussions

3.1 SEM Morphologies of TiO_2, c-TiO_2: AgNPs and c-TiO_2: AgNPs

The SEM surface morphologies of the TiO_2, c-TiO_2: AgNPs and m-TiO_2: AgNPs composite films are shown in figure 1(a-c). The SEM image of TiO_2 shows little difference between films with AgNPs and all films showed compact morphologies and smooth surfaces. As shown, addition of AgNPs lead to enhanced aggregation of the nanoparticles on the surface.

This enhanced property shows that, the film has grown by a cluster mechanism and greater sensitivity to the composition of the sample than was possible without AgNPs. When the unadulterated micrograph of the film is compared with the silver modified surfaces, we observed a microscopic structural change in the films.

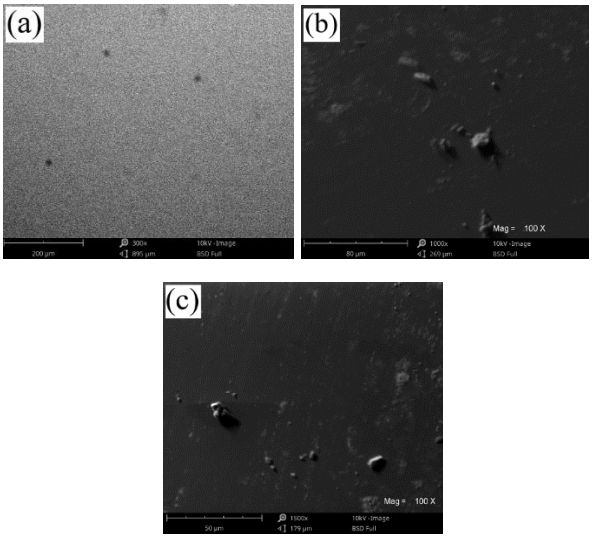

Figure 1: SEM and EDX micrographs of a) TiO_2, b) c-TiO_2: AgNPs and c) m-TiO_2: AgNPs

3.2 Microstructure of TiO_2

Figure 2 shows the XRD pattern of TiO_2 nanoparticles. As shown in the figure, all the peaks of diffraction were indexed with the anatase phase. The pattern shows peaks of diffraction at 25.27°, 38.07°, 47.96°, 54.93° and 66.60° which are indexed to (101), (004), (200), (211) and (213) crystalline planes respectively.

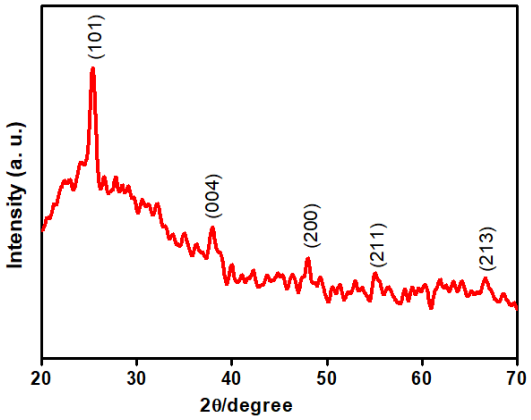

Figure 2: XRD pattern of TiO_2

Their corresponding d-spacing are 4.962, 3.216, 2.893, 3.521 and 1.891 Å. The result obtained for the TiO_2 is in agreement with the anatase phase according to Joint Committee on Powder Diffraction Standards (JCPDS) Card No. 21-1272 and also in line with similar studies [18, 19].

3.3 UV-Visible spectroscopy

Figure 3(a) shows the absorption of the natural pigment that serves as light photosensitizer in this research. It was recorded within the wavelength range of 200 – 1200 nm.

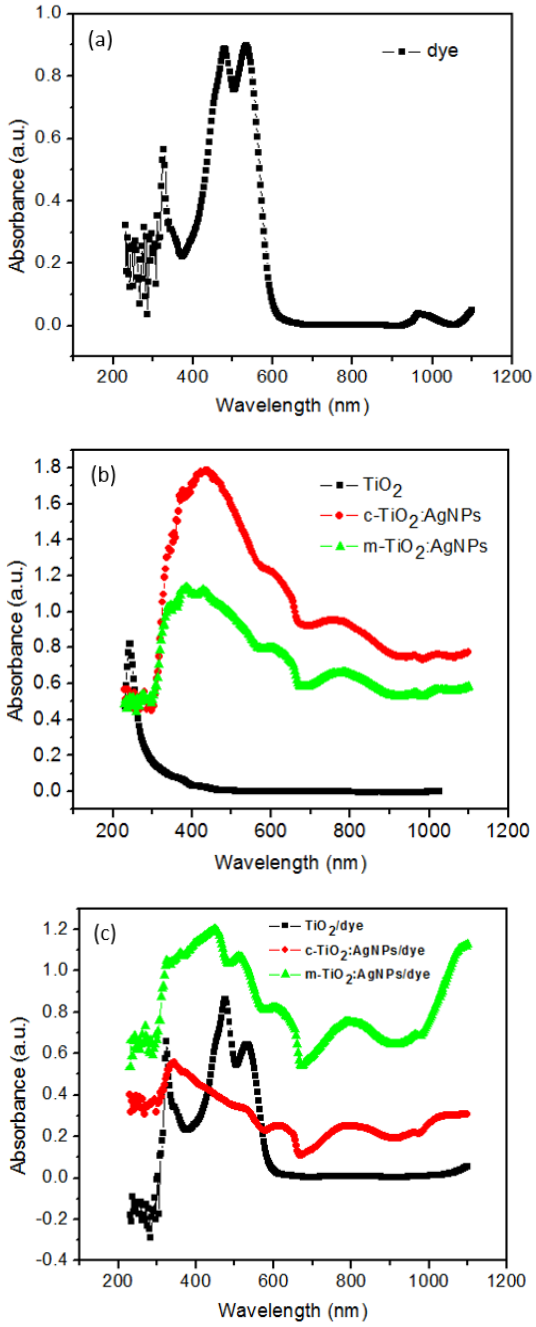

Figure 3: The absorption-wavelength of a) natural pigment, b) TiO_2, c-TiO_2: AgNPs and m-TiO_2: AgNPs without dye and c) TiO_2, c-TiO2: AgNPs and m-TiO_2: AgNPs with dye

From Figure 3(a), the photosensitizer shows absorbing capacity between 400 and 600 nm with two distinct noticeable peaks at ~450 and ~550 nm. This absorption at the visible region shows a satisfactory requirement for the dye pigment in this research.

Figure 3(b) shows the absorbance-wavelength plot for TiO_2, c-TiO_2 and m-TiO_2 without dye pigment. As seen, no absorption peak was seen within the Visible region of TiO_2, but a sharp

peak was observed around 316 nm which falls within the ultraviolet (UV) region. This peak was due to electronic transitions between molecules having an intermediate ionic degree. The absorptivity at the UV region affirmed to the necessity of modifying the TiO_2 to make it active under visible light.

After modification of TiO_2 (compact and mesoporous) with AgNPs, absorption enhancement was noticed on the film. This shows that modification of TiO_2 with AgNPs causes a deformation in the network of the film thereby resulting to redshift in the optical band edge.

Also, peaks were observed between 360 and 850 nm after sensitizing with the natural dye pigment which demonstrate a red shift at the wavelength (figure 3(c)). As shown, the slightly red shifted extinction spectrum of the dye-soaked samples as compared to the un-soaked samples was as a result of the change in the LSPR which slightly shifts to longer wavelength upon the bond formation between the nanoparticles and the dye.

In addition, the absorption intensity increased as the dye was sensitized on the samples. This behavior was usually ascribed to Ag^0 nanoparticles inducing visible light absorption [3, 13, 16]. Moreover, absorption bands at 400–500 nm may also be attributed to Ag clusters.

3.4 *Photovoltaic performance*

DSSCs were fabricated and their behavior were investigated. Their performance parameters were obtained from the Current-voltage (*J-V*) and Power-voltage (*P-V*) curves following equations (1) and (2) respectively [3].

$$FF = \frac{J_{max} \times V_{max}}{J_{SC} \times V_{OC}} \quad (1)$$

$$PCE = \frac{FF \times J_{SC} \times V_{OC}}{P_{IRRADIANCE}}.100\% \quad (2)$$

Where *FF* is Fill Factor, PCE is solar cell efficiency, V_{max} is maximum voltage, J_{max} is maximum current density, J_{sc} is short circuit current density, V_{oc} is open circuit voltage and $P_{IRRADIANCE}$ is light intensity.

Figure 4(a) shows the *J-V* curves of all the DSSCs samples while figure 4(b) shows the *P-V* curves of the formed DSSCs. The individual results are also tabulated in table 1. The unmodified DSSC, i.e., cell without the inclusion of Ag nanoparticles, achieves an efficiency of 0.36%. Its photocurrent density, and open circuit voltage, are 1.89 mA cm^{-2} and 0.45 V respectively. The measured *J-V* curve of the control sample has a fill factor value of 42%.

With the introduction of Ag nanoparticles on TiO_2, the cell's performance improved significantly. Device with AgNPs on c-TiO_2 shows an improved efficiency of 0.64 % while, the best performance was obtained when AgNPs was applied on m-TiO_2.

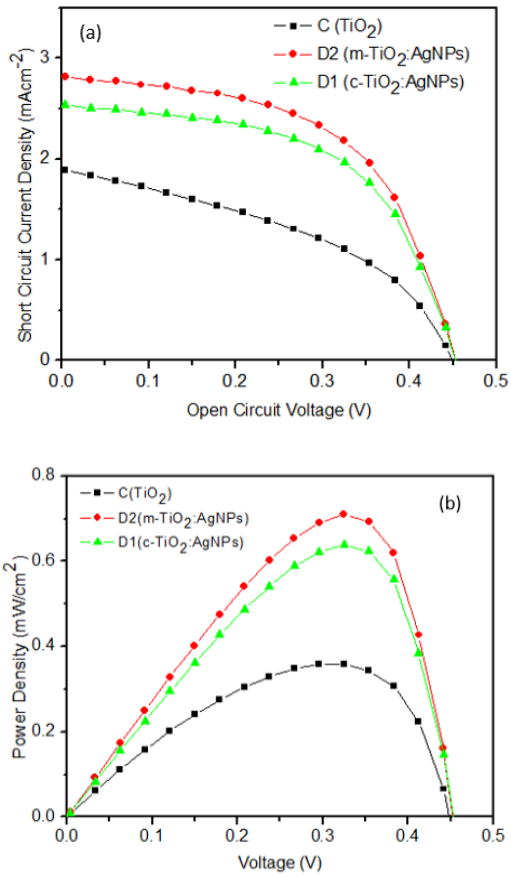

Figure 4: a) J-V curves and b) P-V curves of the control, D1, D2 devices

The measured efficiency for the cell was 0.71% (i.e., ~ 2.0 times improvement compared with that without Ag nanoparticles). The improved PCE was largely because of the increased J_{sc} due to the intensified near field effect resulting from the silver nanoparticles. Addition of AgNPs on the m-TiO_2 creates a Schottky barrier which minimizes recombination due to oxygen vacancies in TiO_2 in the surface layers [13].

Also, the AgNPs plasmon band overlaps energetically with the dye transferring the charge into the TiO_2 nanoparticles. However, when AgNPs is added to c-TiO_2, we also observed an enhancement compared to the reference device but not as pronounced as observed in the device with AgNPs on m-TiO_2. Therefore, cell with AgNPs on m-TiO_2 is the optimum composition in order to get the maximum plasmonic effect of the Ag nanoparticles in our work.

As a result of the decay of a strong LSPR from the AgNPs when it is coated on the c-TiO_2 layer, only limited dye molecules around the porous TiO_2 were stimulated to enhance charge separation and dissociation [14, 16]. This behavior caused a

poor optical absorption of the dye, which subsequently lead to low photocurrent.

Also, the electrons from metal nanoparticles cannot be transported effectively in the network and the study suggests that in such case, specular reflectivity is at high influence, thus stopping a fraction of light to get into the device [13, 14, 21], as such accounts for the low performance.

Table 1: Photovoltaic performance of AgNPs modified and unmodified DSSCs

Device	J_{sc} (mAcm^{-2})	V_{oc} (V)	*FF* (%)	η (%)	Enhancement
Control	1.89	0.45	42	0.36	0
D1	2.53	0.46	55	0.64	~1.80 times
D2	2.83	0.46	54	0.71	~2.00 times

Figure 4(b) shows the *P-V* curves of the control, D1, D2 devices. Their maximum powers are observed at 0.36, 0.64 and 0.71 mWcm^{-2}.

Figure 5 shows the plot of solar cell parameters; V_{oc}, J_{sc}, *FF* and PCE with respect to the device. Observation shows that PCE and J_{sc} maximum values are at 0.71% and 2.83 mAcm^{-2} which was displayed by device D2. Device D1 demonstrates the highest *FF* with value of 0.55.

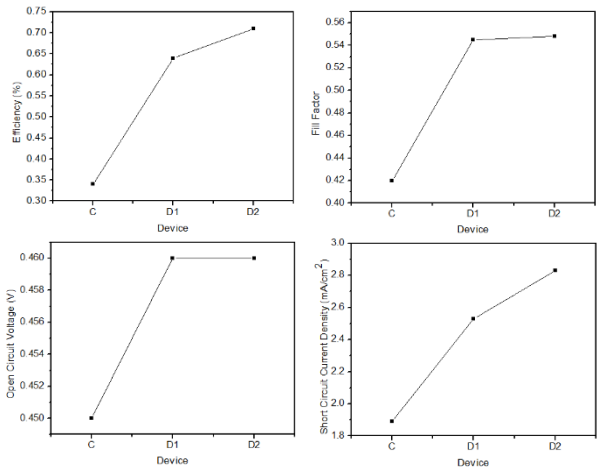

Figure 5: The curve of solar cell parameters; V_{oc}, J_{sc}, FF and PCE with respect to the device

4 Conclusion

The influence of AgNPs on the structure and performance of TiO_2-Ag composite photoanodes and DSSCs was investigated. The results demonstrated that adding AgNPs to TiO_2 photoanodes significantly improved the performance of the DSSCs by increasing short-circuit current and open-circuit voltage. The best performing DSSC has AgNPs on the m-TiO_2 and gave a J_{sc} of 2.83 mAcm^{-2}, a V_{oc} of 0.46 V and a photoelectric conversion efficiency of 0.71%, greatly superior to that of DSSC using pure TiO_2 photoanode. The increase of J_{sc} is attributed to the enhanced light absorption and broadened absorption spectral range of the composite photoanode which is due to the surface plasmon resonance effect of AgNPs.

Acknowledgement

The authors are grateful to Physics Advanced Laboratory, Sheda Science Technology Complex (SHESTCO) and Namiroch research Laboratory, Abuja for the use of their equipment.

Declaration of Competing Interest

Authors have declared that there was no conflict of interest.

References

[1] H. K. Jun, M. A. Careem and A. K Arof, "Quantum dot-sensitized solar cells perspective and recent developments: A review of Cd chalcogenide quantum dots as sensitizers," Renewable and Sustainable Energy Reviews, vol. 22, p. 148, 2013.

[2] C. Dragonetti and A. Colombo, "Recent Advances in Dye-Sensitized Solar Cells," Molecules, vol. 26, p. 2461, 2021.

[3] D. Eli, G. J. Ibeh, O. O. Ige, J. A. Owolabi, R. U. Ugbe, B. O. Sherifdeen, M. Y. Onimisi and H. Ali, "Silver Nanoparticles as Nano Antenna for TiO2 Activation and its Application in DSSC for Enhanced Performance," Journal of Theoretical and Applied Physics, vol. 1, no. 3, p. 88, 2019.

[4] M. Dhonde, K. Sahu, M. Das, A. Yadav, P. Ghosh and V. V. S. Murty, "Review—Recent Advancements in Dye-Sensitized Solar Cells; From Photoelectrode to Counter Electrode," Journal of The Electrochemical Society, vol. 169, no. 6, p. 066507, 2022.

[5] O. Francis and A. Ikenna, "Review of Dye-Sensitized Solar Cell (DSSCs) Development," Natural Science, vol. 13, p. 496, 2021.

[6] I. F. Okoye, A. O. C. Nwokoye and G. Ahmad, "Power Voltage Characteristics of Fabricated Dssc Incorporating Multiple Organic Dyes as Photosensitizer," Energy and Power Engineering, vol. 13, p. 221, 2021.

[7] C. C. Chen, V. S. Nguyen, H. C. Chiu, Y. D. Chen, T. C. Wei and C. Y. Yeh, "Anthracene-Bridged Sensitizers for Dye-Sensitized Solar Cells with 37% Efficiency under Dim Light," Advanced Energy Materials, vol. 12, no. 20, p. 2270080, 2022.

[8] J. M. Ji, H. Zhou, Y. K. Eom, C. H. Kim and H. K. Kim, "14.2% Efficiency Dye-Sensitized Solar Cells by Co-sensitizing Novel Thieno[3,2-b]indole-Based Organic Dyes with a Promising Porphyrin Sensitizer," Advanced Energy Materials, vol. 10, no. 15, p. 2000124, 2020.

[9] D. Devadiga, M. Selvakumar, P. Shetty and M. S. Santosh, "Dye-Sensitized Solar Cell for Indoor Applications: A Mini-Review," Journal of Electronic Materials, vol. 50, p. 3187, 2021.

[10] K. Sharma, V. Sharma and S. S. Sharma, "Dye-Sensitized Solar Cells: Fundamentals and Current Status," Nanoscale Research Letters, vol. 13, p. 381, 2018.

[11] J. J. Yoo, G. Seo, M. R. Chua, T. G. Park, Y. Lu, F. Rotermund Y. K. Kim, C. S. Moon, N. J. Jeon, J. P. Correa-Baena, V. Bulovic, S. S. Shin, M. G. Bawendi and J. Seo, "Efficient perovskite solar cells via improved carrier management," Nature, vol. 590, no. 7847, p. 587, 2021.

[12] Z. Qu, F. Ma, Y. Zhao, X. Chu, S. Yu and J. You, "Updated Progresses in Perovskite Solar Cells," Chinese Physics Letters, vol. 38, no. 10, p. 107801, 2021.

[13] J. J. Yoo, G. Seo, M. R. Chua, T. G. Park, Y. Lu, F. Rotermund Y. K. Kim, C. S. Moon, N. J. Jeon, J. P. Correa-Baena, V. Bulovic, S. S. Shin, M. G. Bawendi and J. Seo, "Efficient perovskite solar cells via improved carrier management," Nature, vol. 590, no. 7847, p. 587, 2021.

[14] R. Selvapriya, T. Abhijith, V. Ragavendran, V. Sasirekha, V. S. Reddy, J. M. Pearce and J. Mayandi, "Impact of coupled plasmonic effect with multishaped silver nanoparticles on efficiency of dye sensitized solar cells," Journal of Alloys and Compounds, vol. 894, p. 162339, 2022.

[15] D. Kabir, T. Forhad, W. Ghann, B. Richards, M. M. Rahman, M. N. Uddin, M. R. J. Rakib, M. H. Shariare, F. I.Chowdhury, M. M. Rabbani, N. M.Bahadur and J. Uddin, "Dye-sensitized solar cell with plasmonic gold nanoparticles modified photoanode," Nano-Structures & Nano-Objects, vol. 26, p. 100698, 2021.

[16] E. Danladi, and P. M. Gyuk, "High efficiency dye sensitized solar cells by excitation of localized surface plasmon resonance of AgNPs," Science World Journal, vol. 14, no. 2, p. 125, 2019.

[17] S. Agnihotri, S. Mukherji, and S. Mukherji, "Size-controlled silver nanoparticles synthesizedover the range 5–100 nm using the same protocol and their antibacterial efficacy," RSC Advances, vol. 4, p. 3974, 2014.

[18] E. Danladi, M. Y. Onimisi, S. Garba, and J. Tasiu, "9.05 % HTM free perovskite solar cell with negligible hysteresis by introducing silver nanoparticles encapsulated with P4VP Polymer," SN Applied Sciences, 2:1769, 2020.

[19] S S. Al-Taweel and H. R. Saud "New route for synthesis of pure anatase TiO2 nanoparticles via ultrasound-assisted sol-gel method," Journal of Chemical and Pharmaceutical Research, vol. 8, no. 2, p. 620, 2016.

[20] S. Li, X. Zhu, B. Wang, Y. Qiao. W. Liu, H. Yang, N. Liu, M. Chen, H. Lu and Y. Yang, "Influence of Ag Nanoparticles with Different Sizes and Concentrations Embedded in a TiO2 Compact Layer on the Conversion Efficiency of Perovskite Solar Cells," Nanoscale Research Letters, vol. 13, no. 210, p. 1, 2018.

[21] G. Zhao, H. Kozuka, and T. Yoko, "Sol-gel preparation and photo-electrochemical properties of TiO2 films containing Au and Ag metal particles," Thin Solid Films, vol. 277, p. 147, 1996.